Applied Ocean Research 73 (2018) 88–99

Contents lists available at ScienceDirect

Applied Ocean Research

journal homepage: www.elsevier.com/locate/apor

Nonparametric identification of nonlinear ship roll motion by using the motion response in irregular waves

Xian-Rui Hou[a], Zao-Jian Zou[b,c,*], Cheng Liu[d]

[a] College of Ocean Science and Engineering, Shanghai Maritime University, Shanghai 201306, China
[b] State Key Laboratory of Ocean Engineering, Shanghai Jiao Tong University, Shanghai, 200240, China
[c] School of Naval Architecture, Ocean and Civil Engineering, Shanghai Jiao Tong University, Shanghai, 200240, China
[d] Navigation College, Dalian Maritime University, Dalian, Liaoning, 116026, China

ARTICLE INFO

Article history:
Received 11 November 2017
Received in revised form 15 January 2018
Accepted 5 February 2018
Available online 21 February 2018

Keywords:
Nonlinear roll motion
Nonparametric identification
Random decrement technique
Support vector regression

ABSTRACT

In order to precisely predict the nonlinear roll motion of ships at sea, it is important to determine the nonlinear damping and restoring moment as accurately as possible. In this paper, a nonlinear mathematical model is used to describe the nonlinear roll motion of ships at sea. A novel nonparametric identification method based on a combination of random decrement technique (RDT) and support vector regression (SVR) is used to identify the nonlinear damping and restoring moments in the mathematical model simultaneously by using only the random rolling responses of ships in irregular waves. In the identification method, RDT is first used to derive the random decrement equation as well as the auto- and cross-correlation equations based on the established mathematical models, and the random decrement signatures are also obtained from the random roll responses. Then SVR is applied to identify the damping and restoring moments in the roll motion equation. For the purpose of verifying the applicability, accuracy and generalization ability of the identification method, it is applied to analyzing the simulated data with different wave excitations. The identification results show that the identification method can be applied to identify the damping and restoring moments of the nonlinear roll motion using the random responses of ships in irregular waves.

1. Introduction

When a ship is navigating at sea, the roll motion has a significant influence on its safety and operability; therefore, it is crucial to predict the roll motion as accurately as possible. In order to predict the roll motion, a universal mathematical model for describing the nonlinear roll motion of ships in waves is usually established according to the rigid body dynamics. The key issue to predict the roll motion of ships precisely is to determine the damping and restoring moments in the mathematical model correctly.

Although the roll damping has been investigated by many researchers for a long time since William Froude in the 19th century, a universal method to predict the damping moment which is mainly dependent on the fluid viscosity is still absent. To predict the roll damping, several methods are available, i.e., model test method [1–3], semi-empirical method [4–6], numerical method based on CFD [7–9] and system identification method.

System identification technique, which aims to find the best mathematical model that relates the output to the input of a system, has been used to identify the roll damping of ships. Ueno et al. [10] applied the improved energy method and the genetic algorithm respectively to estimate the roll damping coefficients and the restoring moment coefficients for fishing boats. Considering the good performance of the nonlinear fitting, artificial neural networks have been used to identify the roll motion of ships by many researchers. Mahfouz [11] applied artificial neural network to identify the roll damping and restoring moment coefficients of ships. Besides, Haddara [12], Xing and McCue [13], Ueno and Fan [14] also used artificial neural networks to identify the roll motion of ships. Kim and Park [15], Kim et al. [16] used Hilbert transform method to identify the nonlinear roll damping and restoring moments of a FPSO by analyzing the free decay test. Somayajula and Falzarano [17] applied R-MISO method to identify the roll parameters of an S-175 container ship. Recently, with the development of the inverse problem theory, it has been used to study the roll motion of ships. Jang et al. [18] applied the deterministic inverse method to identify the functional form of the nonlinear roll damping of ships. Jang [19] improved this method to simultaneously identify the nonlinear damping and the restoring moments of nonlinear sys-

* Corresponding author at: School of Naval Architecture, Ocean and Civil Engineering, Shanghai Jiao Tong University, Shanghai, 200240, China.
E-mail address: zjzou@sjtu.edu.cn (Z.-J. Zou).

https://doi.org/10.1016/j.apor.2018.02.004

tems. Han and Kinoshita [20] presented an application of stochastic inverse method for the nonlinear damping identification and used the method to identify the nonlinear roll damping of a ship.

During the past twenty years, with the rapid development of statistic learning theory and data mining technology, support vector regression (SVR) as a new generation of machine study method has been widely used to solve problems in engineering. SVR is first proposed by Vapnik [21,22] in the 1990s. Compared to the conventional parameter estimation methods such as the least square method, maximum likelihood estimation and artificial neural network which adopt the empirical risk minimum principle and are suitable for large scale samples learning, SVR adopts the structural risk minimum principle and is suitable for small scale samples learning. Luo and Zou [23] first applied the least square SVR to identify the mathematical model of ship maneuvering motion, and the validity of SVR in the parametric identification is validated by the numerical experiment. Zhang and Zou [24], Wang et al. [25] also used SVR to identify the hydrodynamic derivatives in the equations of ship maneuvering motion. Xu et al. [26] used the least square SVR to identify the nonlinear coefficients in the dynamic model of underwater vehicles. In order to predict the roll motion accurately, Hou and Zou [27,28] used SVR to identify the nonlinear damping and restoring moment coefficients by using only the measured roll responses in regular waves and in irregular waves, respectively. From these studies, the robustness and convergence property of SVR are demonstrated and validated.

In the present study, in order to predict the nonlinear roll motion of ships in irregular waves by using the mathematical model, a robust nonparametric identification method based on a combination of random decrement technique (RDT) and SVR is proposed to identify the damping and restoring moments for the nonlinear roll motion of ships in irregular waves by using only the random roll responses. To begin with, a nonparametric mathematical model is established to describe the nonlinear roll motion of ships at sea. Then the random decrement equation as well as the auto- and cross-correlation equations is derived based on the established mathematical model by using RDT, and SVR is used to identify the nonlinear damping and restoring moments in the roll motion equation. In order to validate the applicability, accuracy and the ability of generalization, the proposed method is used to analyzing the simulated responses of a vessel model in irregular waves. Finally, some conclusions are drawn.

2. Equation of roll motion

According to the rigid body dynamics, the roll motion of a ship at sea can be described by a second order nonlinear ordinary differential equation of the form

$$(I_{xx}+J_{xx})\ddot{\phi}+D(\dot{\phi})+R(\phi)=M(t) \tag{1}$$

where ϕ is the roll angle (rad); I_{xx} is the mass moment of inertia (kg m^2); J_{xx} is the added mass moment of inertia (kg m^2); D is the nonlinear damping moment (N m); R is the restoring moment (N m); M is the wave exciting moment (N m).

From Eq. (1), it can be seen that there are four variables to be determined, i.e., J_{xx}, D, R and M. Dividing Eq. (1) by the total mass moment of inertia ($I_{xx}+J_{xx}$), the normalized roll motion equation is obtained

$$\ddot{\phi}+d(\dot{\phi})+r(\phi)=K(t) \tag{2}$$

where $d(\dot{\phi})=D(\dot{\phi})/(I_{xx}+J_{xx})$; $r(\phi)=R(\phi)/(I_{xx}+J_{xx})$; $K(t)=M(t)/(I_{xx}+J_{xx})$. In order to predict the roll damping of a ship in waves accurately, various mathematical models have been proposed [29–32]. The nonlinear damping, as a function of roll rate, can be expressed as a sum of two terms: a linear term and a nonlinear term. Two forms are usually used to describe the nonlinear term, i.e., the quadratic form and the cubic form. In this study, the nonlinear damping is expressed in the form of

$$d(\dot{\phi})=d_1\dot{\phi}+f_1(\dot{\phi}) \tag{3}$$

where d_1 is the linear damping coefficient; the function f_1 denotes the nonlinear component of the damping.

The restoring moment, as an odd function of the roll angle, can be expressed by the Taylor series of the roll angle

$$r(\phi)=c_1\phi+c_3\phi^3+c_5\phi^5+\ldots \tag{4}$$

where c_i (i = 1,3,5,...) is the restoring moment coefficient.

However, the order of the Taylor expansion is usually determined empirically. In the present study, the restoring moment is expressed by

$$r(\phi)=c_1\phi+f_2(\phi) \tag{5}$$

where c_1 is the linear restoring moment coefficient; f_2 denotes the nonlinear component of the restoring moment.

Substituting Eqs. (3) and (5) into Eq. (2), the normalized roll motion equation is rewritten as

$$\ddot{\phi}+d_1\dot{\phi}+c_1\phi+f(\phi,\dot{\phi})=K(t) \tag{6}$$

where $f(\phi,\dot{\phi})=f_1(\dot{\phi})+f_2(\phi)$.

3. Identification method

The identification method consists of two parts: one is RDT which is applied to derive the random decrement equation and obtain the random decrement signatures from the roll responses of a ship in irregular waves; the other is SVR which is applied to identify the nonlinear damping and restoring moments based on the derived random decrement equation and the obtained random decrement signatures.

3.1. Random decrement technique

Random decrement technique (RDT), as an averaging technique, has been successfully applied to system identification in ship and ocean engineering by combining with conventional identification methods [33,34]. The basic concept of RDT is that the random roll response of a ship in irregular waves can be divided into two components: one is the deterministic component which is dependent on the initial state; the other is the random component which is dependent on the external excitation. By using RDT, the random component is removed and the deterministic component of the roll motion, named as the random decrement signature, is kept.

When Eq. (6) is used to describe the roll motion of a ship in irregular waves, the following variable substitutions are used

$$y_1=\phi, \qquad y_2=\dot{\phi}, \qquad Y=[y_1,y_2]^{\mathrm{T}} \tag{7}$$

The wave excitation is assumed to satisfy the following conditions

$$E\left[K(t)\right]=0, \qquad E\left[K(t)K(t+\tau)\right]=\psi_0\delta(\tau) \tag{8}$$

where $E[\cdot]$ denotes the ensemble average of variables; ψ_0 is the variance of the excitation; δ is the Dirac delta function.

Then the random process Y is a Markov process, and its conditional probability density function can be described by virtue of the Fokker-Planck equation

$$\frac{\partial P}{\partial t}=-\frac{\partial}{\partial y_1}(y_2P)+\frac{\partial}{\partial y_2}\left\{\left[d_1y_2+c_1y_1+f(y_1,y_2)\right]P\right\}+\frac{\psi_0}{2}\frac{\partial^2 P}{\partial y_2^2} \tag{9}$$

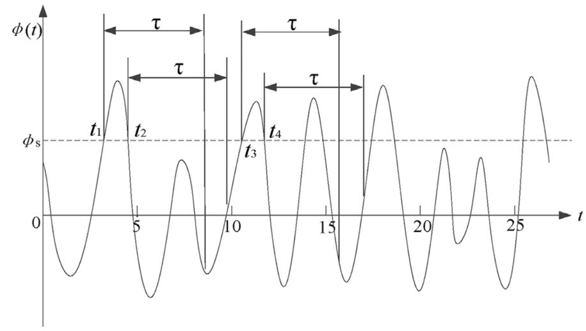

Fig. 1. Illustration of the procedure to obtain random decrement signatures.

where $P = P(y_1, y_2, t \mid y_{1,0}, y_{2,0})$ is the conditional probability density of the random process Y. The solution of Eq. (9) subjects to the following initial condition

$$\lim_{t\to 0} P(y_1, y_2, t|y_{1,0}, y_{2,0}) = \delta(y_1 - y_{1,0})\delta(y_2 - y_{2,0}) \quad (10)$$

where $y_{1,0}$ and $y_{2,0}$ are the initial roll angle and roll rate, respectively.

Multiplying Eq. (9) by the variables y_1 and y_2, respectively, and integrating the equation with respect to these two variables in the interval $[-\infty, \infty]$, the following equation is obtained

$$\begin{cases} \dot{\mu}_1 = \mu_2 \\ \dot{\mu}_2 = -d_1\mu_2 - c_1\mu_1 - f(\mu_1, \mu_2) \end{cases} \quad (11)$$

where $f(\mu_1, \mu_2) = E[f(y_1, y_2)]$; $\mu_1 = E[y_1]$; $\mu_2 = E[y_2]$.

The above formula can be rewritten into a second-order nonlinear differential equation in the form of

$$\ddot{\mu}_1 + d_1\mu_2 + c_1\mu_1 + f(\mu_1, \mu_2) = 0 \quad (12)$$

According to Eq. (6), the free decay equation of the roll motion can be written as

$$\ddot{\phi} + d_1\dot{\phi} + c_1\phi + f(\phi, \dot{\phi}) = 0 \quad (13)$$

Comparing Eq. (12) with Eq. (13), it is obvious that these two equations are similar in the sense that the linear coefficients and the structure of the nonlinear function in these two equations are same. Thus, the linear coefficients and the nonlinear function in Eq. (6) can be determined by use of Eq. (12), which is called the random decrement equation with respect to the nonlinear roll motion equation, Eq. (6). In Eq. (12), μ_1, μ_2 are named as the random decrement signatures of the roll angle and the roll rate, respectively.

Multiplying Eq. (9) by $y_i(t)y_j(t+\tau)P$ ($i = 1, 2$ and $j = 1, 2$) and integrating the whole equation with respect to y_1 and y_2 in the interval $[-\infty, \infty]$, the auto- and cross-correlation functions are obtained:

$$\begin{cases} \dot{R}_{11} = R_{21} \\ \dot{R}_{21} = -d_1R_{21} - c_1R_{11} - E[f(y_1, y_2)y_1(t+\tau)] \\ \dot{R}_{12} = R_{22} \\ \dot{R}_{22} = -d_1R_{22} - c_1R_{12} - E[f(y_1, y_2)y_2(t+\tau)] \end{cases} \quad (14)$$

where R_{11} and R_{22} are the auto-correlation functions of the roll angle and roll rate, respectively; R_{21} and R_{12} are the cross-correlation functions of the roll rate and roll angle, respectively.

From Eq. (12) and Eq. (14), it can be seen that neither of the two equations is used separately to identify the linear damping moment coefficient d_1, the linear restoring moment coefficient c_1 and the nonlinear function $f(y_1, y_2)$ simultaneously. To identify the linear coefficients, remove the last term containing the function $f(y_1, y_2)$ in Eq. (14), it follows

$$\begin{cases} \dot{R}_{21} = -d_1R_{21} - c_1R_{11} \\ \dot{R}_{22} = -d_1R_{22} - c_1R_{12} \end{cases} \quad (15)$$

According to Eq. (15), the linear coefficients d_1 and c_1 can be identified by use of the auto- and cross-correlation functions. Once the coefficients d_1 and c_1 are identified, the nonlinear function $f(y_1, y_2)$ can be identified according to Eq. (12) by using the random decrement signatures.

In order to obtain the random decrement signatures, firstly, a constant roll angle is selected as the trigger value, and N segments of equal length are selected from the roll response, with each segment beginning at the instant at which the value of the roll angle is equal to the selected trigger value, as shown in Fig. 1. The initial slopes of these segments vary alternatively between positive and negative, so that one half of the segments start with the positive slope and the other half start with the negative slope. Note that overlapping which may happen between the sequential segments is allowed. Secondly, each segment is discretized with the same time step and the roll response values at the discrete points are obtained by using the interpolation technique. Then the random decrement signatures are obtained by superposing all the roll response values at the discrete points with the same sequence number and dividing them by the number of segments N.

3.2. Support vector regression

In this subsection, the basic concept of support vector regression (SVR) is briefly introduced, and more details can be found in Cristianini and Shawe-Taylor [35], Smola and Schölkopf [36].

The training samples are assumed to be

$$S = \left\{(x_i, y_i), i = 1, 2, \cdots, l\right\} \in \left(\Re^n \times \Re\right)_l \quad (16)$$

where $x_i \in \Re^n$ is the i^{th} n-dimensional training input vector; $y_i \in \Re$ is the corresponding training output; l is the number of training samples; $\Re^n$ is the n-dimensional Euclidean space and $\Re$ is the set of real numbers.

The goal is to find a feature function $g(x)$ which is often described as

$$g(x) = w^{\mathrm{T}}\Phi(x) + b(x \in \Re^n) \quad (17)$$

where $\Phi(x)$ is a transformation function which transforms the input vector x in the Euclidean space into the vector $X = \Phi(x)$ in the feature space; w is a weight matrix; b is a bias.

According to the statistical learning theory [21], the function estimation problem of finding the feature function in Eq. (17) based on the training samples in Eq. (16) is transformed to a quadratic optimization problem which is described by

$$\begin{aligned} &\min_{w,\ \xi^{(*)}} \ J(w, \xi, \xi^*) = \frac{1}{2}w^{\mathrm{T}}w + C\sum_{i=1}^{l}(\xi_i + \xi_i^*) \\ &\text{Subject to} \quad [\langle w, \Phi(x_i)\rangle + b] - y_i \le \varepsilon + \xi_i \\ &\qquad y_i - [\langle w, \Phi(x_i)\rangle + b] \le \varepsilon + \xi_i^* \\ &\qquad \xi_i, \quad \xi_i^* \ge 0; \quad i = 1, 2, \cdots, l \end{aligned} \quad (18)$$

where C is the penalty parameter; ξ and ξ^* are the slack factor vectors; $\langle\cdot,\cdot\rangle$ denotes the inner product; ε is the insensitive loss parameter.

Define the Lagrange function

$$L_f\left(w,b,\xi,\xi^*;\alpha,\alpha^*,\eta,\eta^*\right)=\frac{1}{2}w^{\mathrm{T}}w+C\sum_{i=1}^{l}\left(\xi_i+\xi_i^*\right)-\sum_{i=1}^{l}\left(\eta_i\xi_i+\eta_i^*\xi_i^*\right)-\sum_{i=1}^{l}$$

$$\alpha_i\left(\varepsilon+\xi_i+y_i-\langle w,\phi(x_i)\rangle-b\right)-\sum_{i=1}^{l}\alpha_i^*\left(\varepsilon+\xi_i^*-y_i+\langle w,\phi(x_i)\rangle+b\right) \tag{19}$$

where $\alpha_i,\quad \alpha_i^*,\quad \eta_i,\quad \eta_i^*\geq 0$ are the Lagrange multipliers.

According to the dual theorem, by introducing the Lagrange function, the primal quadratic optimization problem in Eq. (18) is transformed into the problem of solving the saddle point of the Lagrange function, i.e.,

$$\max_{\alpha,\alpha^*,\eta,\eta^*}\quad\min_{w,b,\xi,\xi^*}\quad L_f\left(w,b,\xi,\xi^*;\alpha,\alpha^*,\eta,\eta^*\right) \tag{20}$$

The procedure for solving Eq. (20) consists of two steps: in the first step, the minimum value of the Lagrange function L_f is solved and a new quadratic optimization problem, as the dual problem of the primal quadratic optimization problem in Eq. (18), is deduced; in the second step, the dual optimization problem is solved by use of the suitable numerical algorithms to obtain the optimal solution, and the optimal solution of the dual optimization problem is equal to the optimal solution of the primal optimization problem in Eq. (18).

The partial derivatives of L_f with respect to the primal variables (w,b,ξ_i,ξ_i^*) have to vanish for optimality. It follows

$$\begin{cases}\dfrac{\partial L_f}{\partial w}=0\rightarrow w=\displaystyle\sum_{i=1}^{l}\left(\alpha_i^*-\alpha_i\right)\Phi(x_i)\\ \dfrac{\partial L_f}{\partial b}=0\rightarrow\displaystyle\sum_{i=1}^{l}\left(\alpha_i-\alpha_i^*\right)=0\\ \dfrac{\partial L_f}{\partial \xi_i}=0\rightarrow\eta_i=C-\alpha_i\\ \dfrac{\partial L_f}{\partial \xi_i^*}=0\rightarrow\eta_i^*=C-\alpha_i^*\end{cases} \tag{21}$$

Substituting Eq. (21) into Eq. (20), the dual problem of the primal optimization in Eq. (18) is obtained

$$\min_{\alpha,\alpha^*}\quad W(\alpha,\alpha^*)=\frac{1}{2}\sum_{i=1}^{l}\sum_{j=1}^{l}(\alpha_i^*-\alpha_i)(\alpha_j^*-\alpha_j)$$

$$K(x_i,x_j)+\varepsilon\sum_{i=1}^{l}(\alpha_i^*+\alpha_i)-\sum_{i=1}^{l}y_i(\alpha_i^*-\alpha_i) \tag{22}$$

$$\text{Subject to}\quad\sum_{i=1}^{l}(\alpha_i-\alpha_i^*)=0,\quad\alpha_i,\ \alpha_i^*\in[0,\quad C]$$

where K is the kernel function matrix and its element $K(x_i,x_j)$ equals to the inner product of the two input vectors in the feature space, i.e., $K(x_i,x_j)=\langle\Phi(x_i),\Phi(x_j)\rangle$.

Substituting Eq. (21) into Eq. (17), the feature function of SVR is transformed into

$$g(x)=\sum_{i=1}^{n}(\alpha_i^*-\alpha_i)K(x_i,x)+b \tag{23}$$

To solve the convex quadratic programming problem in Eq. (22), any kind of optimization algorithms for solving quadratic programming problem can be applied. In this study, in order to improve the training efficiency of SVR, a novel numerical algorithm, called sequential minimum optimization (SMO) algorithm [37,38], is applied to solve the dual optimization problem. Compared with the traditional optimization algorithms for quadratic programming, the greatest merit of the SMO algorithm is to train SVR analytically instead of invoking a time-consuming numerical quadratic programming optimizer explicitly. The SMO algorithm consists of the following steps:

1) Initialize the Lagrange multipliers $\alpha_k,\ \alpha_k^*,\ k=1,2,\cdots,l$ and the bias b with arbitrary value;
2) By applying the heuristics search, two Lagrange multipliers which violate the optimality conditions in Eq. (21) are picked out to construct the smallest quadratic programming problem

$$W(\lambda_i,\lambda_j)=\sum_{k=1,\,k\neq i,j}^{l}\lambda_k\lambda_iK(x_k,x_i)+\sum_{k=1,\,k\neq i,j}^{l}\lambda_k\lambda_jK(x_k,x_j)$$

$$+\frac{1}{2}\lambda_i^2K(x_i,x_i)+\lambda_i\lambda_jK(x_i,x_j)+\frac{1}{2}\lambda_j^2K(x_j,x_j)+\varepsilon|\lambda_i|+\varepsilon|\lambda_j|-y_i\lambda_i-y_j\lambda_j \tag{24}$$

where $\lambda_k=\alpha_k^*-\alpha_k$;

3) Based on the optimal solution of Eq. (24), the bias b and the output error of SVR are updated respectively, then go to step 2) until all the Lagrange multipliers satisfy the optimality conditions. If no two Lagrange multipliers can be optimized, the training process is finished.

4. Roll motion identification

In this section, the proposed method based on a combination of RDT and SVR is applied to identify the nonlinear damping and restoring moments in the roll motion equation of ships by using only the random responses in irregular waves.

Firstly, the auto- and cross-correlation functions are calculated and the random decrement signatures are obtained from the random roll responses. The auto- and cross-correlation functions are calculated by

$$R_{ij}(\tau)=\frac{1}{N_p-\tau}\sum_{k=1}^{N_p-\tau}y_i(k)y_j(k+\tau) \tag{25}$$

where N_p is the total number of measured data in the roll responses.

In order to extract the random decrement signatures from the roll responses, the significant value of the roll angle, i.e., the arithmetic mean of the one-third maximum roll angle, is selected as the trigger value of the random decrement signatures.

Secondly, Eq. (15) is integrated in the interval $[t_n, t_{n+1}]$ and the integrals of the two terms in the right hand side of the equation are solved by using the trapezoidal method, it follows

$$\begin{cases}R_{21}(n+1)-R_{21}(n)=-\dfrac{hd_1}{2}\left[R_{21}(n+1)+R_{21}(n)\right]-\dfrac{hc_1}{2}\left[R_{11}(n+1)+R_{11}(n)\right]\\ R_{22}(n+1)-R_{22}(n)=-\dfrac{hd_1}{2}\left[R_{22}(n+1)+R_{22}(n)\right]-\dfrac{hc_1}{2}\left[R_{12}(n+1)+R_{12}(n)\right]\end{cases} \tag{26}$$

where $R_{ij}(n)$ $(i,j=1,2)$ are the auto- or cross-correlation functions at the n^{th} time step; h is the time step size.

The training samples for identifying the linear coefficients by SVR with respect to the first and second formulae in Eq. (26) are constructed as

$$\begin{aligned}&\text{Input}\quad=\left\{\ R_{21}(n+1)+R_{21}(n);\quad R_{11}(n+1)+R_{11}(n)\ \right\}\\ &\text{Output}=\left\{\ R_{21}(n+1)-R_{21}(n)\ \right\}\end{aligned} \tag{27}$$

$$\begin{array}{ll} \text{Input} & = \left\{ R_{22}(n+1)+R_{22}(n); \quad R_{12}(n+1)+R_{12}(n) \right\} \\ \text{Output} & = \left\{ R_{22}(n+1)-R_{22}(n) \right\} \end{array} \tag{28}$$

Based on the constructed training samples set in Eqs. (27) and (28), SVR is trained by the SMO algorithm. Therein, the penalty parameter C and the insensitive loss parameter ε are determined by the trial-and-error method. Considering that Eq. (26) is linear with respect to the unknown coefficients, the linear inner product function is selected as the kernel function of SVR:

$$K(x, \quad x') = \langle x, \quad x' \rangle = x^{\mathrm{T}} \cdot x' \tag{29}$$

Compared Eq. (26) with the feature function of SVR in Eq. (23), once SVR has been trained, i.e., the bias b approximates to zero; then $\sum_{i=1}^{l}(\alpha_i^* - \alpha_i)x_i$ is the identified linear coefficients.

Thirdly, by the numerical differentiation, Eq. (12) is discretized as

$$f(\mu_{1,n}, \mu_{2,n}) = -\frac{\mu_{2,n+1} - \mu_{2,n}}{h} - d_1^i \mu_{2,n} - c_1^i \mu_{1,n} \tag{30}$$

where $f(\mu_{1,n}, \mu_{2,n})$ denotes the value of the function at the n^{th} time step; d_1^i is the identified linear damping coefficient; c_1^i is the identified linear restoring moment coefficient.

According to Eq. (30), the training samples set for the nonlinear function identification by SVR is constructed as

$$\begin{array}{ll} \text{Input} & = \left\{ \mu_{1,n}; \quad \mu_{2,n} \right\} \\ \text{Output} & = \left\{ \dfrac{\mu_{2,n} - \mu_{2,n+1}}{h} - d_1^i \mu_{2,n} - c_1^i \mu_{1,n} \right\} \end{array} \tag{31}$$

When SVR is applied to identify the unknown nonlinear function $f(y_1, y_2)$, the Gauss radial basis function is selected as the kernel function of SVR. The Gauss basis kernel function is expressed as

$$K\left(x, x'\right) = \exp\left(-\|x - x'\|^2 / 2\sigma^2\right) \tag{32}$$

where σ is the width parameter of the kernel function and is determined together with the penalty parameter C and the insensitive loss parameter ε by the trial-and-error method.

Comparing Eq. (23) with Eq. (30), once SVR has been trained, the trained SVR model can be used as the identified nonlinear function $f(y_1, y_2)$.

Finally, substituting the identified linear coefficients and the identified nonlinear function into the roll motion equation of ships and solving the roll motion equation by the fourth-order Runge-Kutta method, the nonlinear roll motion of ships in waves can be predicted.

The flow chart of the identification procedure is shown in Fig. 2.

In order to verify the accuracy, validity and generalization ability of the identification method, it is applied to analyzing the simulation data which are obtained by using different mathematical model with different wave excitations.

For the purpose of verification, two mathematical models with different damping expressions are used to generate the random responses. The first mathematical model, in which the damping is expressed as the sum of the linear and quadratic terms in the roll rate, is given as [39]

$$\ddot{\phi} + 0.1627\dot{\phi} + 0.5214\dot{\phi}|\dot{\phi}| + 11.4921\phi + 1.7008\phi^3 = K(t) \tag{33}$$

The second mathematical model, in which the damping is expressed as the sum of the linear and the cubic terms in the roll rate, is given as [12]

$$\ddot{\phi} + 0.32\dot{\phi} + 0.16\dot{\phi}^3 + 16\phi + 19.20\phi^3 = K(t) \tag{34}$$

In these mathematical models, the white noise and the JONSWAP spectrum are taken as the external excitation, respectively.

Table 1
Parameters of SVR for the linear coefficient identification.

Simulation model	White noise excitation	JONSWAP spectrum excitation
Eq. (33)	$C = 10^8$, $\varepsilon = 0.05$	$C = 10^6$, $\varepsilon = 0.05$
Eq. (34)	$C = 10^7$, $\varepsilon = 0.05$	$C = 10^7$, $\varepsilon = 0.05$

For the white noise excitation, the wave exciting moment is assumed to be composed of 70 sinusoidal components of constant amplitude 0.07 rad/s^2. The frequency range of the excitation is taken between 2.0 and 5.0 rad/s. The wave exciting moment is expressed as

$$K(t) = \sum_{i=1}^{70} 0.07\cos(\omega_i t + \theta_i) \tag{35}$$

where ω_i is the frequency of the wave excitation component; θ_i, as a random variable uniformly distributed between 0 and 2π, is the phase shift among these wave excitation components.

For the JONSWAP spectrum excitation, the wave exciting moment is also assumed to be composed of 70 sinusoidal components of variable amplitudes. The significant value and the modal frequency of the wave exciting moment are assumed to be 0.07 rad/s^2 and 3.14 rad/s, respectively. The frequency range of the excitation is taken between 2.0 and 8.0 rad/s. The wave exciting moment is expressed as

$$K(t) = \sum_{i=1}^{70} A_i \cos(\omega_i t + \theta_i), \quad A_i = \sqrt{2S(\omega_i)\Delta\omega} \tag{36}$$

where A_i is the amplitude of the wave excitation component; $S(\omega)$ is the spectrum density; $\Delta\omega$ is the frequency increment.

Using the fourth-order Runge-Kutta method with the time step size 0.05s, the random roll responses are simulated. The results obtained by solving Eqs. (33) and (34) are shown in Figs. 3 and 4, respectively.

According to Eq. (25), the auto- and cross-correlation functions are calculated based on the simulated responses. The results are shown in Figs. 5 and 6, respectively.

Based on the simulated responses, the random decrement signatures of the roll motion can be obtained by RDT. When the random decrement signatures of the roll motion are obtained from the simulated responses using Eq. (33), the trigger value of the random decrement signatures is selected as $\phi_s = 0.136$ rad for the white noise excitation and $\phi_s = 0.112$ rad for the JONSWAP spectrum excitation, respectively. When the random signatures of the roll motion are obtained from the simulated responses using Eq. (34), the trigger value of the random decrement signatures is selected as $\phi_s = 0.120$ rad for the white noise excitation and $\phi_s = 0.069$ rad for the JONSWAP spectrum excitation, respectively. The obtained random decrement signatures are shown in Figs. 7 and 8, respectively.

Firstly, based on the auto- and cross-correlation functions, the training samples set for the linear coefficient identification are constructed according to Eq. (27) and Eq. (28) and then used to train SVR by the SMO algorithm. The penalty parameter C and the insensitive loss parameter ε of SVR are determined by the trial-and-error method. The results are given in Table 1. The training results of SVR are shown in Figs. 9 and 10. In these figures, ΔR_{21} represents the output of the constructed training samples set.

From Figs. 9 and 10, it can be seen that the training samples set are described accurately by the trained SVR.

After SVR is trained, the bias b in the feature function of the trained SVR is obtained, as given in Table 2. From this table, it can be clearly seen that the bias b in every case approximates to zero. Therefore, when SVR is used to identify the linear damping coeffi-

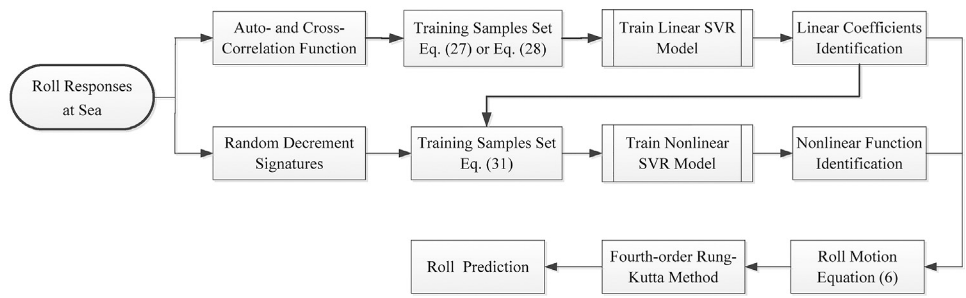

Fig. 2. Flow chart of the identification procedure.

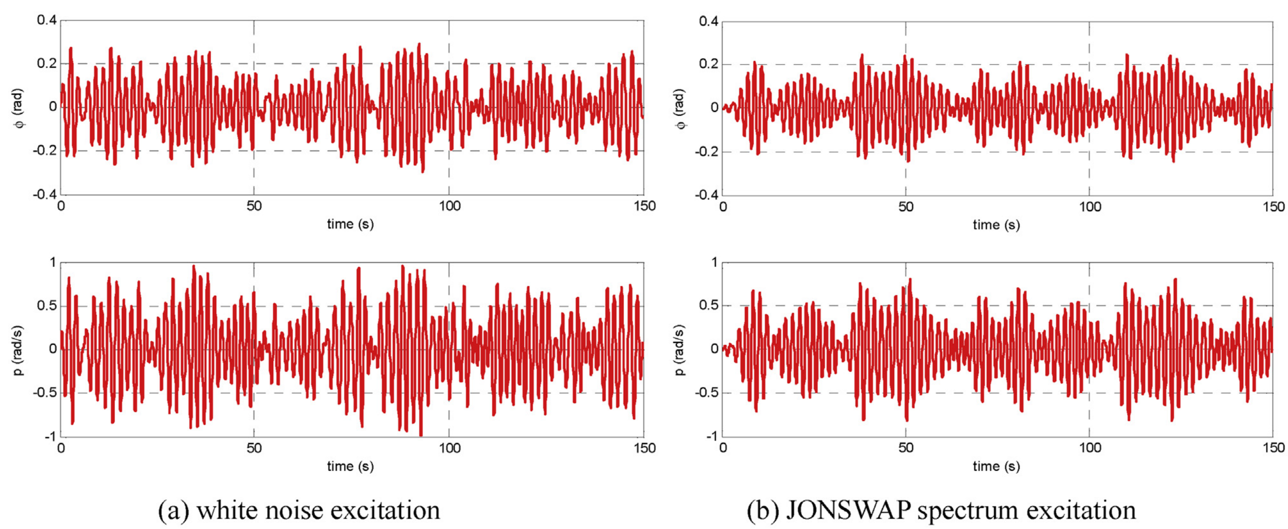

Fig. 3. Simulated roll responses, Eq. (33).

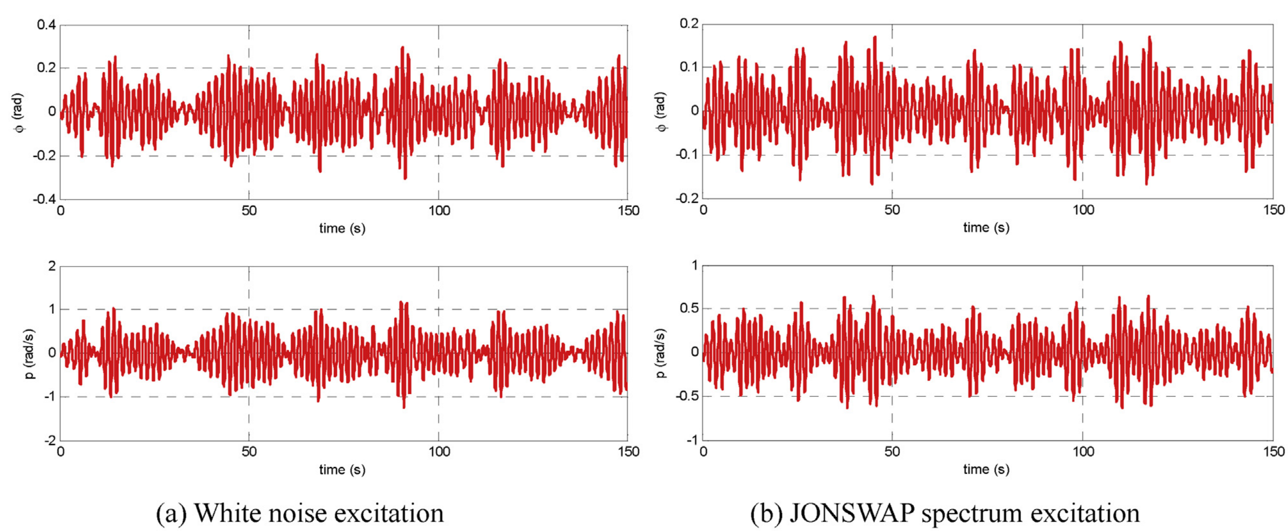

Fig. 4. Simulated roll responses, Eq. (34).

Table 2
Values of the bias b for the linear coefficient identification.

Simulation model	White noise excitation	JONSWAP spectrum excitation
Eq. (33)	$b = -2.49 \times 10^{-5}$	$b = -1.20 \times 10^{-5}$
Eq. (34)	$b = -1.82 \times 10^{-5}$	$b = -8.06 \times 10^{-6}$

cient d_1 and the restoring moment coefficient c_1, the bias b can be ignored without decreasing the identification accuracy. The identified linear damping and restoring moment coefficients are given in Tables 3 and 4 in comparison with the known values, respectively.

From Tables 3 and 4, it is found that the linear restoring moment coefficient is identified accurately while larger discrepancies exist for the linear damping coefficient between the identified values and the known values. The reason is that the linear coefficients are identified based on Eq. (15) instead of Eq. (14). Since the nonlinear

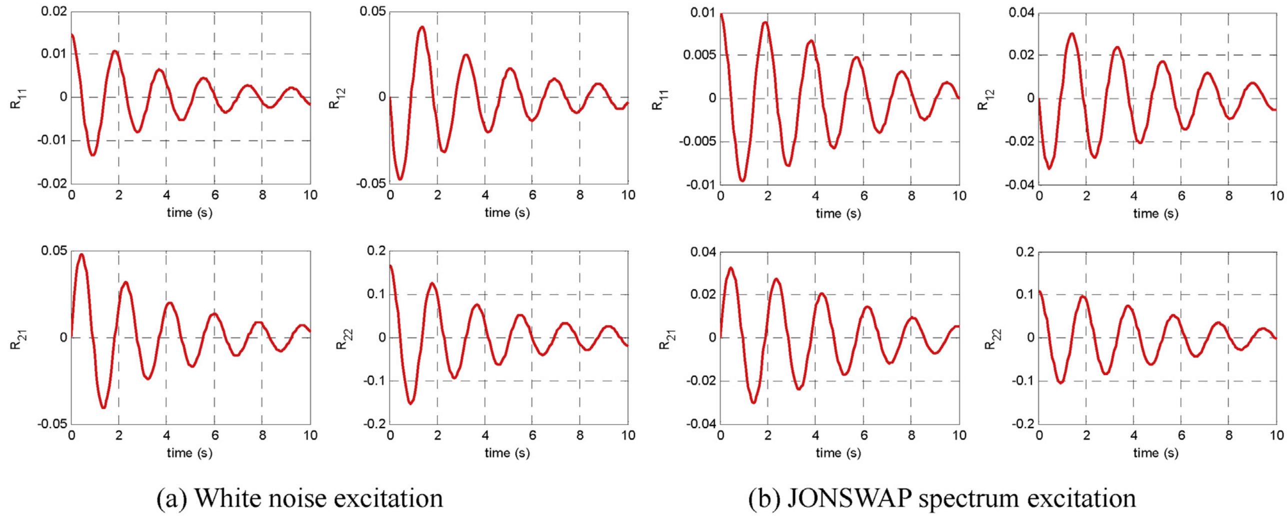

Fig. 5. Auto- and cross-correlation functions of the simulated responses, Eq. (33).

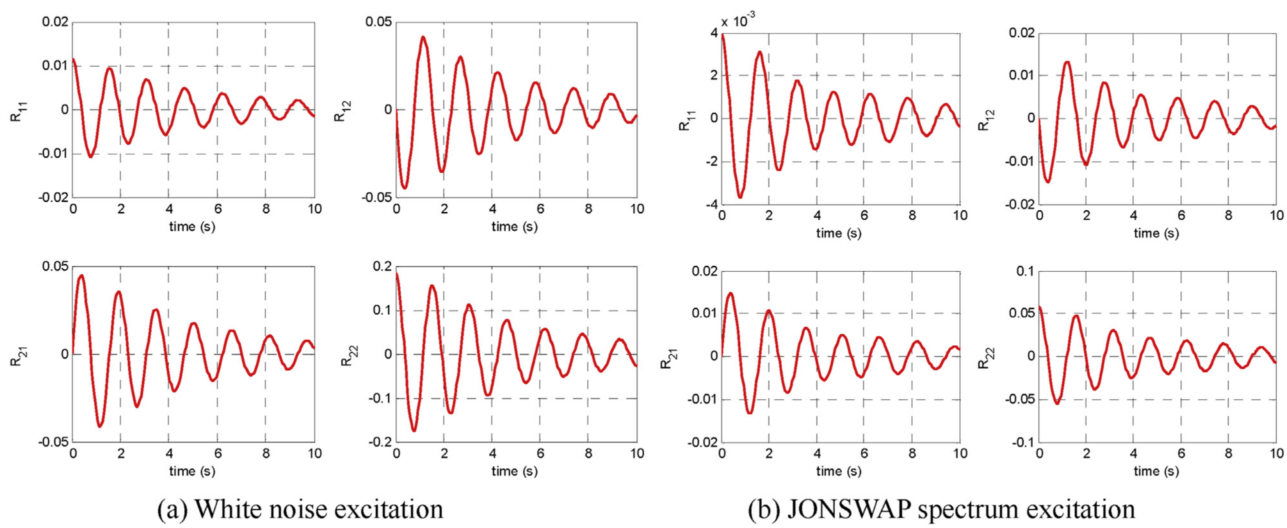

Fig. 6. Auto- and cross-correlation functions of the simulated responses, Eq. (34).

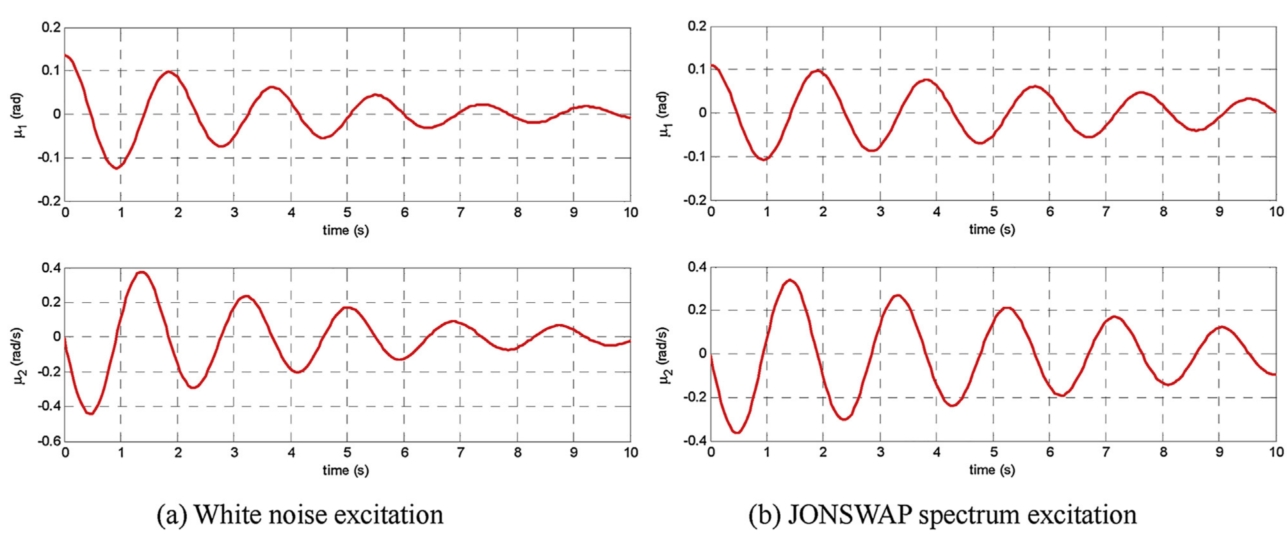

Fig. 7. Random decrement signatures of the simulated responses, Eq. (33).

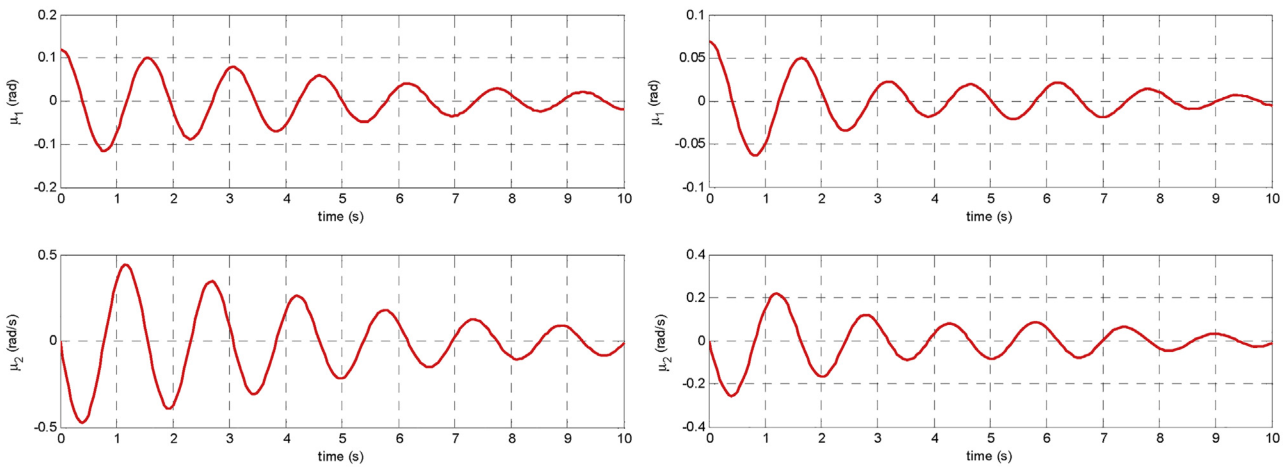

(a) White noise excitation (b) JONSWAP spectrum excitation

Fig. 8. Random decrement signatures of the simulated responses, Eq. (34).

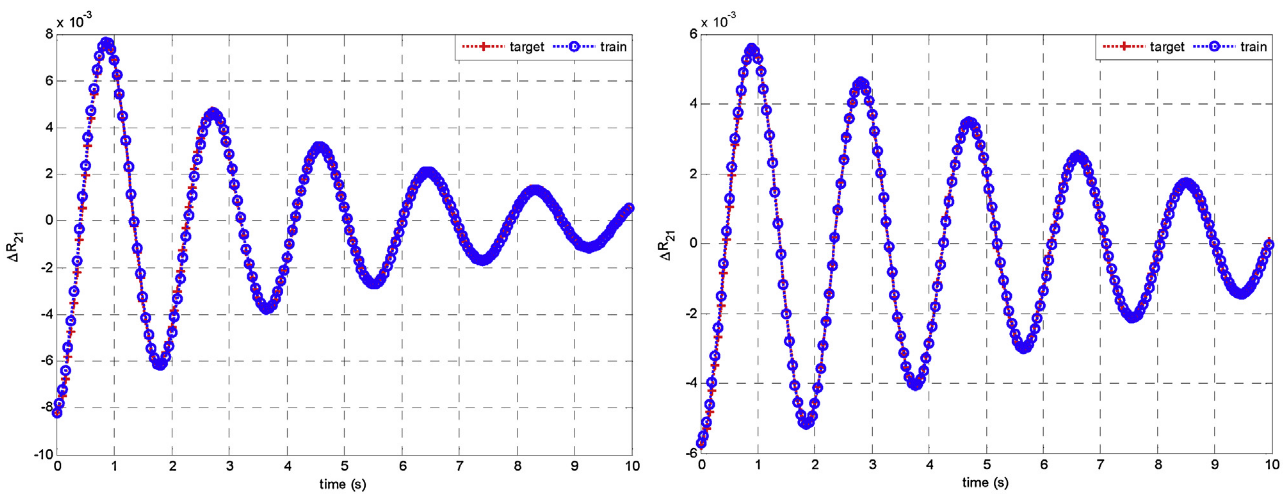

(a) White noise excitation (b) JONSWAP spectrum excitation

Fig. 9. Training results of SVR for linear coefficient identification, Eq. (33).

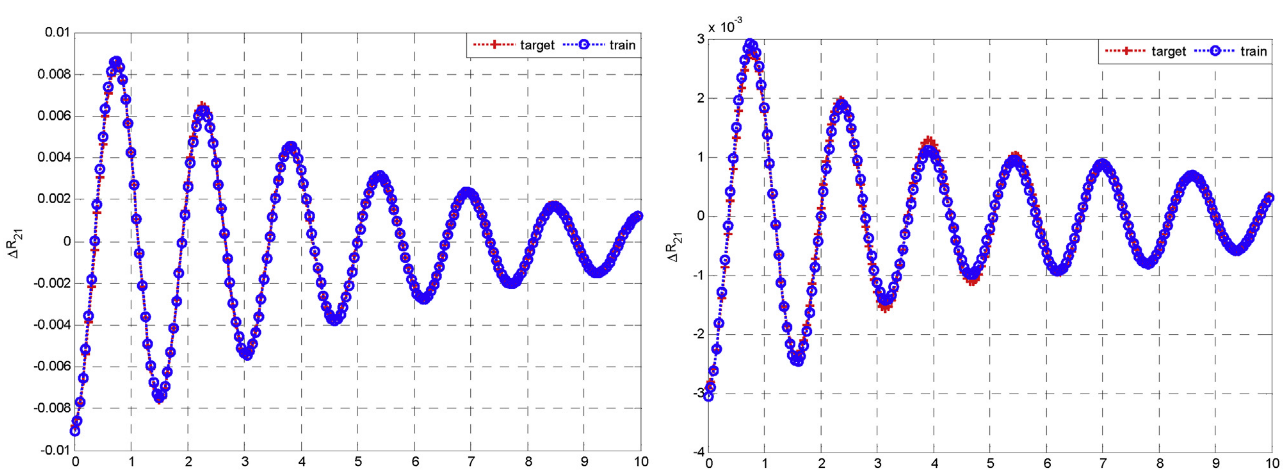

(a) White noise excitation (b) JONSWAP spectrum excitation

Fig. 10. Training results of SVR for linear coefficient identification, Eq. (34).

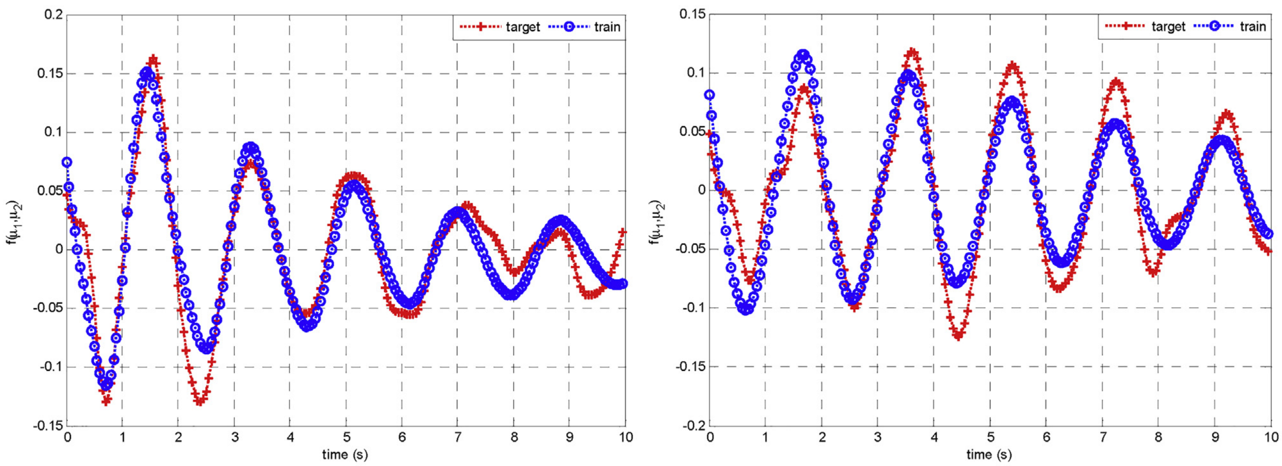

(a) White noise excitation (b) JONSWAP spectrum excitation

Fig. 11. Training results of SVR for nonlinear function identification, Eq. (33).

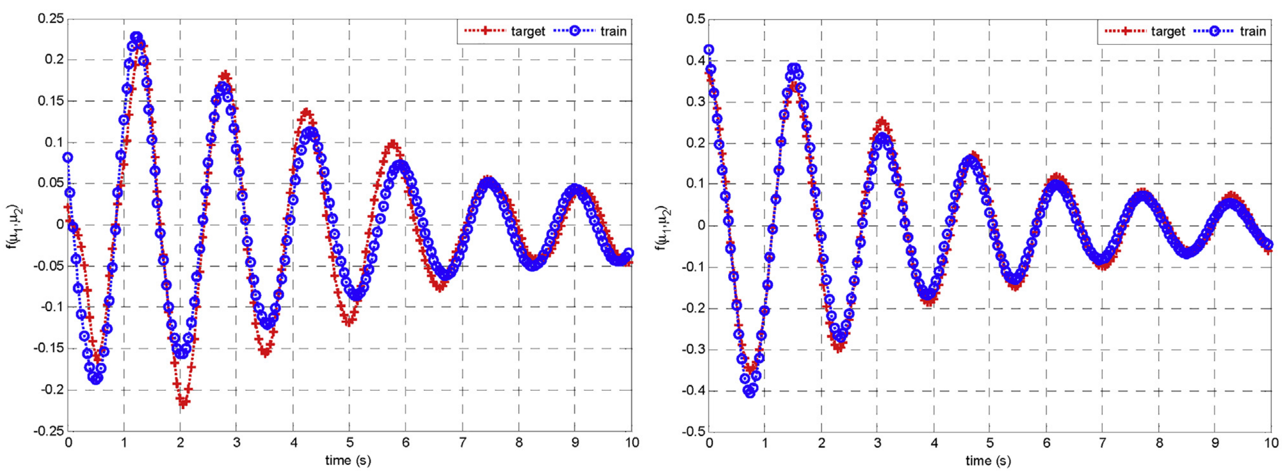

(a) White noise excitation (b) JONSWAP spectrum excitation

Fig. 12. Training results of SVR for nonlinear function identification, Eq. (34).

Table 3
Comparison between the identified values and the known values, Eq. (33).

Coefficient	Known	White noise excitation		JONSWAP spectrum excitation	
		Identified	Error (%)	Identified	Error (%)
d_1	0.1627	0.2864	76.03	0.2249	38.23
c_1	11.4921	11.4991	0.0609	10.9523	4.697

Table 4
Comparison between the identified values and the known values, Eq. (34).

Coefficient	Known	White noise excitation		JONSWAP spectrum excitation	
		Identified	Error (%)	Identified	Error (%)
d_1	0.32	0.35	9.375	0.38	18.75
c_1	16	16.54	3.375	15.50	3.125

Table 5
Parameters of SVR for the nonlinear function identification.

Simulation model	White noise excitation	JONSWAP spectrum excitation
Eq. (33)	$C=1$, $\varepsilon=0.05$, $\sigma=1.5$	$C=1$, $\varepsilon=0.05$, $\sigma=5$
Eq. (34)	$C=1$, $\varepsilon=0.05$, $\sigma=2.5$	$C=1$, $\varepsilon=0.05$, $\sigma=7.5$

function $f(y_1, y_2)$ is removed in Eq. (15) compared to Eq. (14), the identified mathematical model is not exact.

Secondly, substituting the identified linear damping and restoring moment coefficients into Eq. (31), the training samples set for nonlinear function identification are constructed based on the obtained random decrement signatures. Using the trial-and-error method, the penalty parameter C, the insensitive loss parameter ε, and the width parameter σ of the Gauss basis kernel function in Eq. (32) are determined. The results are given in Table 5.

Then the constructed training samples set are used to train SVR by the SMO algorithm. The training results of SVR are shown in Figs. 11 and 12, respectively. From these figures, it can be seen that though some phase differences exist between the target values and the training values for the two mathematical model, the generally satisfactory agreements between these target values and the training values of SVR are achieved. The reasons for the phase differences may be that the constructed kernel function and the selected parameters of SVR (the insensitive loss parameter ε, the penalty parameter C and the width parameter σ of the kernel func-

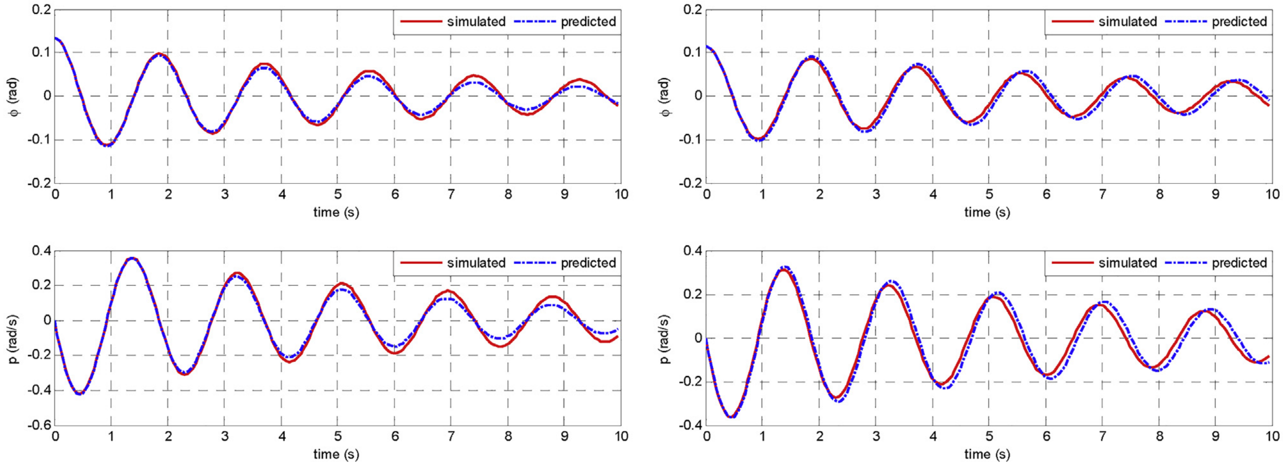

(a) White noise excitation (b) JONSWAP spectrum excitation

Fig. 13. Comparison of the free roll decay motions predicted by Eq. (37) and simulated by Eq. (33).

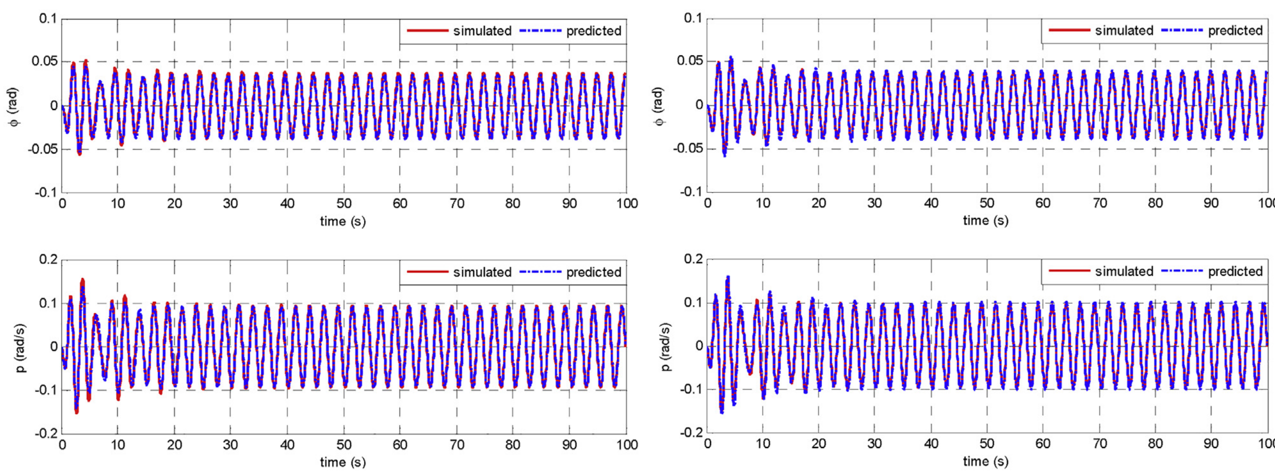

(a) White noise excitation (b) JONSWAP spectrum excitation

Fig. 14. Comparison of the roll motions in regular waves predicted by Eq. (37) and simulated by Eq. (33).

tion) are not optimal, therefore, the training results of SVR cannot completely match the target values.

Finally, substituting the identified linear damping coefficient d_1, the linear restoring moment coefficient c_1 and the trained SVR model of the nonlinear function $f(y_1, y_2)$ into Eq. (6), it follows

$$\ddot{\phi} + d_1^i \dot{\phi} + c_1^i \phi + \mathrm{SVR}_f(\phi, \dot{\phi}) = K(t) \tag{37}$$

where SVR_f is the trained SVR model of the nonlinear function $f(y_1, y_2)$.

Using Eq. (37) and choosing the wave excitation $K(t) = 0$ for the free roll decay test and $K(t) = 0.2\sin(2.5t + \pi)$ for the test in regular waves, the roll motion is predicted with the linear coefficients and the nonlinear function identified by using white noise excitation and JONSWAP spectrum excitation. The results are shown in Figs. 13–16 in comparison with the simulated responses based on the known linear coefficients and nonlinear function. From these figures, it is found that the agreements between the predicted and simulated motions are generally satisfactory. It demonstrates that the identification errors of the linear damping and restoring moment coefficients are compensated in the process of the nonlinear function identification. Therefore, it can be concluded that the proposed identification method based on the combination of RDT and SVR is capable of identifying the damping and restoring moments in Eq. (6) by analyzing the simulated roll motion responses of ships in irregular waves. On the other hand, it also shows that some discrepancies exist between the predicted motions and the simulated ones in these figures. This is due to the training errors existed in the trained SVR model, as shown in Figs. 11 and 12. Therefore, to identify the damping and restoring moments more accurately, the SVR model for the nonlinear function identification should be further improved by constructing the optimal kernel function and selecting the optimal parameters of SVR.

5. Conclusions

In this paper, a mathematical model, in which the nonlinear damping and restoring moments are expressed in the form of the linear term plus the nonlinear term, is established to describe the nonlinear roll motion of ships at sea. To predict the roll motion of ships in irregular waves using the established model, a novel nonparametric identification method which consists of RDT and SVR is proposed to identify the damping and restoring moments in the mathematical model. In this nonparametric identification

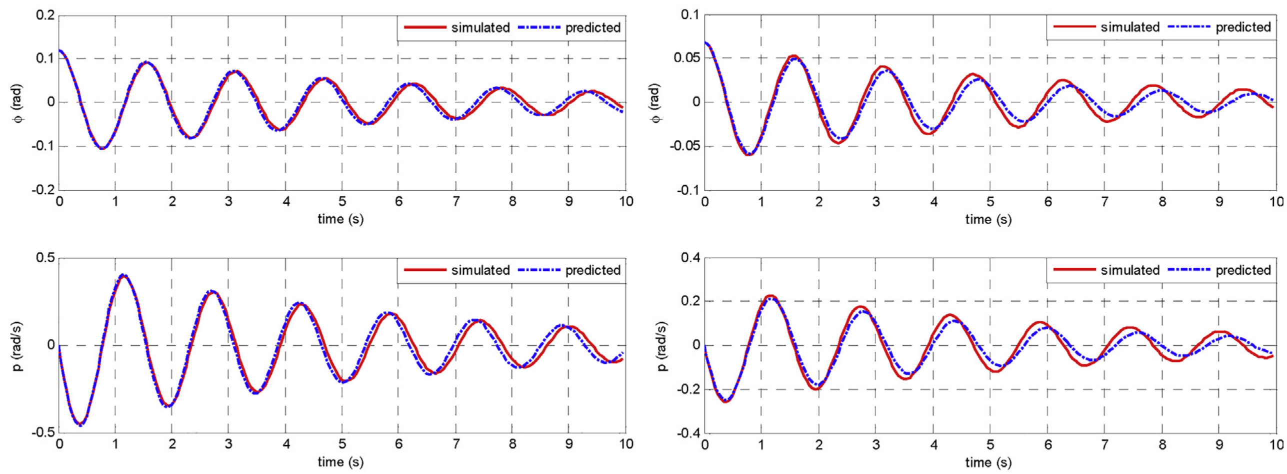

(a) White noise excitation (b) JONSWAP spectrum excitation

Fig. 15. Comparison of the free roll decay motions predicted by Eq. (37) and simulated by Eq. (34).

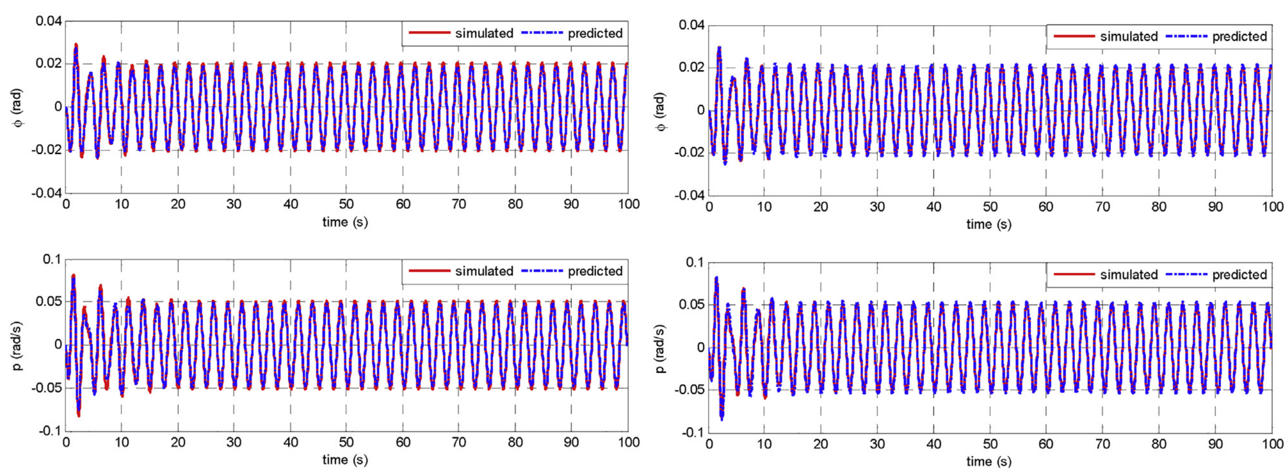

(a) White noise excitation (b) JONSWAP spectrum excitation

Fig. 16. Comparison of the roll motions in regular waves predicted by Eq. (37) and simulated by Eq. (34).

method, RDT is applied to derive the random decrement equation as well as the auto- and cross-correlation equations based on the established mathematical model, and to obtain the random decrement signatures from the random roll responses; SVR is applied to identify the linear coefficients and the nonlinear function. In order to verify the applicability and validity of the identification method, case studies based on the simulation data using two different mathematical models with different wave excitations are carried out, respectively. The satisfactory agreement between the predicted responses using the identified model and the simulated responses using the simulation model indicates that the proposed nonparametric identification method can be effectively applied to identify the nonlinear damping and restoring moments by analyzing the simulated data. Therefore, it can be concluded that the proposed nonparametric identification method, as a complementary method to model test method and numerical method, can be applied to identify the damping and restoring moments for the nonlinear roll motion of ships by only using the random roll response in irregular waves.

However, in the present study the proposed nonparametric identification method is only used to analyze the simulation data. The accuracy and the generalization ability of the nonparametric identification method in analyzing experimental data need to be verified in the future study. Moreover, the focus will be on improving the identification method to make it be able to identify the wave exciting moment for the nonlinear roll motion of ships at sea in the future study.

Acknowledgements

This work is supported by the National Natural Science Foundation of China (Grant No. 51509193) and the Fund of the State Key Laboratory of Ocean Engineering of Shanghai Jiao Tong University for Independent Researches (Grant No. GKZD010056-8).

References

[1] P.T.T. Esperança, J.S. Sales Jr., S.S. Liapis, J.P.J. Matsuura, An experimental investigation of roll motions of an FPSO, in: Proceedings of the ASME 27th International Conference on Offshore Mechanics and Arctic Engineering, Estoril, Portugal, 2008.
[2] O.A. Seelis, L.B. Tao, Experimental determination of roll damping coefficient for FPSO, in: Proceedings of the ASME 33rd International Conference on Ocean, Offshore and Arctic Engineering, California, USA, 2014.
[3] C.S. Kwon, J. Kim, W. Jung, et al., Determination of roll damping coefficients for an FPSO through model tests and CFD analysis, in: Proceedings of the 25th

International Ocean and Polar Engineering Conference, Hawaii, USA, 2015, pp. 1656–1665.
[4] Y. Himeno, Prediction of Ship Roll Damping-State of the Art, Ann Harbor, University of Michigan, College of Engineering, Department of Naval Architecture and Marine Engineering, 1981 (No. 239).
[5] Y. Ikeda, Prediction methods of roll damping of ships and their application to determine optimum stabilization devices, Mar. Technol. 41 (2) (2004) 89–93.
[6] Y. Kawahara, K. Maekawa, Y. Ikeda, A simple prediction formula of roll damping of conventional cargo ships on the basis of Ikeda's method and its limitation, J. Shipp. Ocean Eng. 2 (4) (2012) 201–210.
[7] R.V. Wilson, P.M. Carrica, F. Stern, Unsteady RANS method for ship motions with application to roll for a surface combatant, Comput. Fluids 35 (2006) 501–524.
[8] G.O.G. Avalos, J.B. Wanderley, A.C. des, A.C. Oliveira, Roll damping decay of a FPSO with bilge keel, Ocean Eng. 87 (2014) 111–120.
[9] B. Ommani, T. Kristiansen, R. Firoozkoohi, Nonlinear roll damping, a numerical parameter study, in: Proceedings of the 25th International Ocean and Polar Engineering Conference, Hawaii, USA, 2015, pp. 196–203.
[10] K. Ueno, N. Kimura, K. Amagai, Estimation of coefficients of the equation of nonlinear roll motion for fishing boats by improved energy method and genetic algorithm, Jpn. J. Ind. Appl. Math. 20 (2003) 155–192.
[11] A.B. Mahfouz, Identification of the nonlinear ship rolling motion equation using the measured response at sea, Ocean Eng. 31 (2004) 2139–2156.
[12] M.R. Haddara, Complete identification of the roll equation using the stationary random roll response, J. Ship Res. 50 (4) (2006) 388–397.
[13] Z.L. Xing, L. McCue, Modeling ship equations of roll motion using neural networks, Nav. Eng. J. 122 (3) (2010) 49–60.
[14] K. Ueno, C. Fan, Numerical experiment of ship roll motion by using self-generating radial basis functions network (In Japanese), Jpn. Soc. Ind. Appl. Math. 23 (2) (2013) 287–306.
[15] Y. Kim, M.J. Park, Identification of the nonlinear roll damping and restoring moment of a FPSO using Hilbert transform, Ocean Eng. 109 (2015) 381–388.
[16] Y. Kim, M.J. Park, J.H. Lee, A study on the nonlinear roll behavior of a FPSO using Hilbert transform, in: Proceedings of the Twenty-Sixth International Ocean and Polar Engineering Conference, Rhodes, Greece, 2016, pp. 561–567.
[17] A. Somayajula, J. Falzarano, Estimation of roll motion parameters using R-MISO system identification technique, in: Proceedings of the Twenty-Sixth International Ocean and Polar Engineering Conference, Rhodes, Greece, 2016, pp. 568–574.
[18] T.S. Jang, S.H. Kwon, J.H. Lee, Recovering the functional form of the nonlinear roll damping of ships from a free-decay experiment: an inverse formulism, Ocean Eng. 37 (2010) 1337–1344.
[19] T.S. Jang, Non-parametric simultaneous identification of both the nonlinear damping and restoring characteristics of nonlinear systems whose dampings depend on velocity alone, Mech. Syst. Signal Process. 25 (2011) 1159–1173.
[20] S.L. Han, T. Kinoshita, Stochastic inverse modeling of nonlinear roll damping moment of a ship, Appl. Ocean Res. 39 (2012) 11–19.
[21] V.N. Vapnik, Statistical Learning Theory, John Wiley and Sons, New York, 1998.
[22] V.N. Vapnik, An overview of statistical learning theory, IEEE Trans. Neural Netw. 10 (5) (1999) 988–999.
[23] W.L. Luo, Z.J. Zou, Parametric identification of ship maneuvering models by using support vector machines, J. Ship Res. 53 (1) (2009) 19–30.
[24] X.G. Zhang, Z.J. Zou, Estimation of the hydrodynamic coefficients from captive model test results by using support vector machines, Ocean Eng. 73 (2013) 25–31.
[25] X.G. Wang, Z.J. Zou, F. Xu, et al., Sensitivity analysis and parametric identification for ship manoeuvring in 4 degrees of freedom, J. Mar. Sci. Technol. 19 (2014) 394–405.
[26] F. Xu, Z.J. Zou, J.C. Yin, et al., Identification modeling of underwater vehicles' nonlinear dynamics based on support vector machine, Ocean Eng. 67 (2013) 68–76.
[27] X.R. Hou, Z.J. Zou, SVR-based identification of nonlinear roll motion equation for FPSOs in regular waves, Ocean Eng. 109 (2015) 531–538.
[28] X.R. Hou, Z.J. Zou, Parameter identification of nonlinear roll motion equation for floating structures in irregular waves, Appl. Ocean Res. 55 (2016) 66–75.
[29] D.W. Bass, M.R. Haddara, Nonlinear models of ship roll damping, Int. Shipbuild Progr. 35 (401) (1988) 5–24.
[30] E.B. Malta, R.T. Goncalves, F.T. Matsumoto, et al., Damping coefficient analyses for floating offshore structures, in: Proceedings of the 29th International Conference on Ocean, Offshore and Arctic Engineering, Shanghai, China, 2010.
[31] A.C. de Oliveira, A.C. Fernandes, An empirical nonlinear model to estimate FPSO with extended bilge keel roll linear equivalent damping in extreme seas, in: Proceedings of the ASME 31st International Conference on Ocean, Offshore and Arctic Engineering, Rio de Janeiro, Brazil, 2012.
[32] A.C. de Oliveira, A.C. Fernandes, The nonlinear roll damping of a FPSO hull, J. Offshore Mech. Arct. Eng. 136 (011106) (2014) 1–10.
[33] A.A. Elshafey, M.R. Haddara, H. Marzouk, Identification of the excitation and reaction forces on offshore platforms using the random decrement technique, Ocean Eng. 36 (2009) 521–528.
[34] Y. Kim, S.G. Park, Wet damping estimation of the scaled segmented hull model using the random decrement technique, Ocean Eng. 75 (2014) 71–80.
[35] N. Cristianini, J. Shawe-Taylor, An Introduction to Support Vector Machines and Other Kernel-based Learning Methods, Cambridge University Press, New York, 2000.
[36] A.J. Smola, B. Schölkopf, A tutorial on support vector regression, Stat. Comput. 14 (2004) 199–222.
[37] G.W. Flake, S. Lawrence, Efficient SVM regression training with SMO, Mach. Learn. 46 (2002) 271–290.
[38] N. Takahashi, J. Guo, T. Nishi, Global convergence of SMO algorithm for support vector regression, IEEE Trans. Neural Netw. 19 (6) (2008) 971–982.
[39] X. Wu, Roll Motion Parameter Identification Using Response in Random Waves. Master Thesis, Memorial University of Newfoundland, Newfoundland, Canada, 1992.